# Hemoglobin can attenuate hydrogen peroxide-induced oxidative stress by acting as an antioxidative peroxidase

Widmer, C C ; Pereira, C P ; Gehrig, P ; Vallelian, F ; Schoedon, G ; Buehler, P W ; Schaer, D J

DOI: https://doi.org/10.1089/ars.2009.2826

ANTIOXIDANTS & REDOX SIGNALING
Volume 12, Number 2, 2010

DOI: 10.1089/ars.2009.2826



# Hemoglobin Can Attenuate Hydrogen Peroxide–Induced Oxidative Stress by Acting as an Antioxidative Peroxidase

Corinne C. Widmer,[1] Claudia P. Pereira,[1] Peter Gehrig,[2] Florence Vallelian,[1] Gabriele Schoedon,[1] Paul W. Buehler,[3] and Dominik J. Schaer[1]

## Abstract

Hemoglobin is considered a potentially toxic molecule when released from erythrocytes during hemolysis, inflammation, or tissue injury. The mechanisms of toxicity involve reduced nitric oxide bioavailability and oxidative processes both occurring at the heme prosthetic groups. When the endogenous oxidant $H_2O_2$ reacts with Hb, transient radicals are generated during the peroxidative consumption of $H_2O_2$. If not neutralized, these radicals can lead to tissue toxicity. The net biologic effect of extracellular Hb in an $H_2O_2$-rich environment will therefore be determined by the balance of $H_2O_2$ decomposition (potential protective effect) and radical generation (potential damaging effect). Here we show that Hb can protect different cell types from $H_2O_2$-mediated cell death and the associated depletion of intracellular glutathione and ATP. Importantly, Hb blunts the transcriptional oxidative-stress response induced by $H_2O_2$ in human vascular smooth muscle cells (VSMCs). Based on spectrophotometric and quantitative mass spectrometry analysis, we suggested a novel mechanism in which Hb redox-cycles $H_2O_2$ and simultaneously internalizes the radical burden, with irreversible structural globin changes starting with specific amino acid oxidation involving the heme proximate $\beta$Cys93 and ultimately ending with protein precipitation. Our results suggest that complex interactions determine whether extracellular Hb, under certain circumstances, acts a protective or a damaging factor during peroxidative stress conditions. *Antioxid. Redox Signal.* 12, 185–198.

## Introduction

HEMOGLOBIN (Hb) is released from red blood cells (RBCs) during intravascular hemolysis or on extravasation and subsequent lysis of RBCs during micro- or macroscopic tissue injury. Extracellular Hb has been implicated in the pathogenesis of hemolytic diseases such as sickle cell anemia or malaria and also in more localized processes such as in atherosclerosis with associated intraplaque hemorrhage (1, 6, 8, 18, 22, 35). Two major processes have been explored to explain the pathophysiologic activity of Hb. The neutralization of nitric oxide by the dioxygenase reaction is likely to be involved in the vasoconstrictive and hypertensive properties of Hb (34). Peroxidative properties of Hb, when it reacts with physiologic oxidants such as hydrogen peroxide, have been advocated to propagate oxidative cell and tissue damage. The *in vivo* examples of the oxidative activity of Hb can be found with large intravascular Hb exposures, which cause lipid peroxidation and subsequent lipid peroxide protein modification in the kidneys of exposed animals (4). The excretion of oxidatively modified Hb in the urine of these animals suggests that Hb is directly involved in the processes leading to parenchymal damage (7). In addition, free heme or Hb oxidation products or both have been shown to propagate inflammatory reactions and to enhance cellular susceptibility to oxidative stress (3, 17, 24).

The oxidative toxicity of Hb or myoglobin (Mb) has been associated with the generation of protein radicals, which are formed when ferric ($Fe^{3+}$) Hb reacts with $H_2O_2$ in the following reaction: $\text{Hb-Fe}^{3+} + H_2O_2 \rightarrow {}^{\bullet}\text{Hb-Fe}^{4+}=O + H_2O$ (32, 33). While $H_2O_2$ is consumed during this reaction, the formed radicals can abstract hydrogen atoms from the environment and thereby initiate oxidative damage. In cell cultures, the reaction of ferric myoglobin or some chemically modified Hbs with low and continuous concentrations of $H_2O_2$ enhanced apoptosis compared with the effect of $H_2O_2$ or myoglobin alone (12, 13). Under physiologic conditions, however, it is unlikely that intravascular or extravascular Hb is exclusively in its ferric oxidative state when subjected to $H_2O_2$. Therefore, the more complicated and less well established reaction of ferrous or a mixed ferric/ferrous Hb reaction with $H_2O_2$ might be a more realistic process *in vivo*. In

[1]Division of Internal Medicine, University Hospital, and [2]Functional Genomics Center Zurich, University of Zurich and Swiss Federal Institute of Technology, Zurich, Switzerland.
[3]Center for Biologics Evaluation and Research (CBER), U.S. Food and Drug Administration, Bethesda, Maryland.

the initial reaction of ferrous Hb, $H_2O_2$ is consumed, resulting in the formation oxo-ferryl Hb (Hb-Fe = O). No heme- or protein-located radical is formed during this initial reaction. The reactions of ferrous Hb with $H_2O_2$ can be summarized as follows (9, 21, 28–30).

$$\text{(I) Hb-Fe}^{2+} + H_2O_2 \rightarrow \text{Hb-Fe}^{4+}=O + H_2O$$

$$\text{(IIa) Hb-Fe}^{4+}=O + H_2O_2 \rightarrow \text{Hb-Fe}^{3+}\text{---}O_2^{\cdot -} + 2H^+$$

$$\rightarrow \text{Heme degradation}$$

$$\rightarrow \text{Crosslinking}$$

$$\text{(IIb) Hb-Fe}^{4+}=O + \rightarrow \text{Hb-Fe}^{3+}\text{ (autoreduction to ferric Hb)}$$

$$\text{(IV) Hb-Fe}^{3+} + H_2O_2 \rightarrow {}^{+\cdot}\text{Hb-Fe}^{4+}=O^{2-} + H_2O$$

The biologic consequences of a heme-protein reaction in $H_2O_2$-rich environments are likely a result of the balance of $H_2O_2$ consumption (antioxidative protection) and, conversely, the production of free radicals (oxidative damage). However, in light of the cytotoxic nature of the reaction of $H_2O_2$ with Mb and with some chemically modified Hbs (developed as blood substitutes), the $H_2O_2$ consumption or peroxidase activity has not been considered an intrinsic antioxidant activity of Hb. We recently found extensive heme degradation, $\alpha$-globin cross-linking, and a specific pattern of $\beta$-globin amino acid oxidations that result from the reaction of ferrous Hb with $H_2O_2$ (7, 21, 42). These structural changes occurring during the reaction of Hb with $H_2O_2$ are likely a result of heme-derived radicals reacting with globin amino acids and porphyrin, respectively. In theory, these reactions could "absorb" a significant amount of radical-derived oxidative impact and thereby protect the physiologic environment.

In this study, we found that cell-free Hb can protect different cell types from $H_2O_2$-induced oxidative stress and associated cell damage. The extensive oxidative modification of Hb, which involves globin-chain amino acid oxidation and protein precipitation, is compatible with a protective activity of Hb involving "internalization" of heme-associated oxidative processes.

## Materials and Methods

Glucose oxidase (GOX; 200 units/mg protein or more) and catalase (4,000–8,000 units/mg protein) from *Aspergilus niger* were obtained from Sigma (St. Louis, MO). Different GOX/catalase concentrations were achieved by dilution of the stock solution directly into the appropriate medium. Highly purified hemoglobin (HbA0; purity >99%, referred to as Hb) was provided by Hemosol, Inc. (Toronto, Ontario, Canada) and stored at –80°C until the time of use. This ultrapure Hb has been characterized extensively and is free of catalase (5). For experiments using cell impedance measurements, an essentially catalase-free stroma-free human Hb was used (provided to P.W.B. by Dr. Andre Palmer, Dept. of Chemical and Biomolecular Engineering, The Ohio State University). AcriGlow 301 was purchased from Capricorn (Portland, ME). Amplex Ultra Red Hydrogen Peroxide Assay Kit was purchased from Molecular Probes (Invitrogen, Basel, Switzerland).

### *Measurement of $H_2O_2$ production*

Production of $H_2O_2$ by GOX in the cell-culture medium was measured by adding 0.5 $\mu$l AcriGlow 301 to the reaction. Luminescence was measured intermittently in 5-s readings for the indicated time period with a Lumat Lb 9507 Luminometer (Berthold Technologies, Regensdorf, Switzerland) at room temperature (RT). $H_2O_2$ accumulation in cell-culture supernatants was measured by using the Amplex Ultra Red assay according to the manufacturer's directions. In brief, 50 $\mu$l of cell-culture supernatant was mixed with the reaction solution containing 10 m*M* Amplex Ultra Red and 10 U/ml horseradish peroxidase in microplates. Absorbance (560 nm) was measured in a Multi-Detection Microplate Reader (SpectraMax M2; Bucher Biotec, Basel, Switzerland) after 30 min of incubation at RT, protected from light. The presence of Hb in cell culture did not affect $H_2O_2$ concentrations after ultrafiltration and did not change the assay results.

### *Analysis of hemoglobin oxidation*

Spectral analysis of ferrous and ferric $HbA_0$ (Hemosol Corp., Toronto, Ontario, Canada) was performed by using a Hewlett-Packard HP-8453 rapid-scanning diode-array spectrophotometer (Agilent Technologies, Rockville, MD). Experiments were performed in sealed cuvettes equilibrated at room temperature at 37°C with 50 $\mu$*M* Hb (ferrous and ferric) cell-culture medium containing 4.5 g/dl glucose with (+) and without (–) calf serum and 10 mU of glucose oxidase (GOX; type X-S derived from *Aspergillus niger*, 100,000–250,000 U/g solid material; Sigma Chemical). Initial spectra were obtained before the addition of 10 mU of GOX, and then spectra were measured every 2 min for 2 h over a wavelength range of 450–700 nm. To determine the redox state of ferric and ferrous Hb over a 2-h period, 50 $\mu$*M* of each Hb was diluted in glucose-rich medium with a baseline sample taken and analyzed before the addition of GOX. After the initial sample, 10 mU of GOX was added, and each tube was placed in a 37°C water bath. Samples were removed and analyzed spectrophotometrically at time 0 (immediately after the addition of GOX) and then every 2 min for 30 min, followed by every 10 min (remaining 1.5 h). Each sample was analyzed before and immediately after the addition of 2 m*M* sodium sulfide ($Na_2S$) as a measure of ferryl Hb. The concentration of sulfhemoglobin was calculated by using the extinction coefficient 10.5 per mm at 620 nm and expressed as ferryl Hb (16).

### *Cell culture*

Human vascular smooth muscle cells (VSMCs) were freshly isolated from human umbilical cord veins as described (25). VSMCs (passage three through six) were cultured in DMEM high glucose (4 mg/ml of glucose), without phenol red (Amimed, BioConcept, Allschwil, Switzerland) with 10% FCS, 1% L-glutamine (200 m*M*), 1% penicillin (10,000 U/ml), and streptomycin (10,000 U/ml). RAW 264.7 and HEK-293 cultivated in DMEM high glucose with 10% FCS and additional 2 m*M* L-glutamine. All cells were kept at 37°C in a humidified atmosphere with 5% $CO_2$. All GOX experiments were performed at reduced FCS concentrations (5%). The experiments with HEK293 cells, shown in Fig. 2, were performed under serum-free conditions. All media were without phenol red.

### *Cell-impedance measurements*

Cell-impedance measurements to monitor adherence, spreading, proliferation, detachment, and cell death in real

time were accomplished by using the CELLligence RTCA-SP system (Roche Applied Science, Rotkreuz, Switzerland). HEK293 cells were seeded in 96-well e-plates at a density of ~50,000 cells per well, and the indicated stimuli (in serum-free medium) were added after reaching a stable plateau phase at a normalized cell index (CI) of ~1.0. Data of each well were recorded every 5 min. The measurement was intermittently paused to inspect cells with the microscope. Data were analyzed by using RTCA Software 1.2 (Roche Applied Science).

### *Measurement of intracellular-reduced glutathione and adenosine triphosphate*

Intracellular glutathione (GSH) and adenosine triphosphate (ATP) levels were measured in 96-well cell-culture microplates by using the luminescence GSH-Glo and cell-viability assays from Promega, according to the manufacturer's instructions. Luminescence was measured with an integration time of 0.5 s per well with a Multi-Detection Microplate Reader.

### *RNA isolation and quantitative real-time polymerase chain reaction*

Total RNA was purified with the RNAeasy mini kit (Qiagen, Basel, Switzerland). RNA used for microarray analysis was treated with a DNase I digestion step (Qiagen). RNA was quantified spectrophotometrically by using the Nanodrop ND-1000 spectrophotometer (NanoDrop Technologies, Wilmington, DE). Real-time two-step reverse transcription (RT)-polymerase chain reaction (PCR) was performed on a Fast Real-Time PCR System Instrument (Applied Biosystems, Rotkreuz, Switzerland) by using Taqman reverse transcription and SYBR Green master mix PCR reagents (Applied Biosystems, Roche, Switzerland). Melting-curve analysis was performed after each PCR experiment to show the specificity of amplification reactions and to exclude excessive primer-dimer formation. Temperature-cycling profiles were 10 min at 95°C, 45 cycles of 15 s at 95°C, 10 s at 55–67°C, and 13 s at 72°C. Gene-specific quantitative data were corrected for HPRT RNA abundance in the respective sample and are expressed as fold-expression in relation to the nontreated control (40). Gene-specific primers were as follows: HPRT: 5′-CCAGT CAACAAG-3′ and 5′-CACAATCAAGAC-3′; HO-1: 5′-AG GGTGATAGAAGAGGCCAAGACT-3′ and 5′-TTCCACCG-GACAAAGTTCATGGC-3′; TFR1: 5′-TAAACCTGCTGTTGG GGTTC-3′ and 5′-TGCAGGTCTGACAGGTTCTG-3′; ATF3: 5′-CAAGTGCATCTTTGCCTCAA-3′ and 5′-CCACCCGAG GTACAGACACT-3′; and GDF15: 5′-CTCCAGATTCCGAG AGTTGC-3′ and 5′-AGAGATACGCAGGTGCAGGT-3′

### *Gene-array experiments*

Gene-expression profiling was performed by competitive dual-color hybridization of complementary RNA probes on human 4×44 K oligonucleotide microarray chips (Agilent Technologies, Palo Alto, CA), as described (37). To verify integrity, each RNA sample was analyzed on an RNA 6000 Nanochip (Bioanalyzer 2100 instrument, Agilent Technologies, Basel, Switzerland). High-quality total RNA typically had an 18/28S ribosomal RNA ratio >1.5. cRNA probes were synthesized from 200-ng aliquots of high-quality total RNA by using the low-input fluorescence linear amplification kit protocol and spiked with control targets (Agilent Technologies). Cyanine-3-dCTP (control) or cyanine-5-dCTP (treatment) labeled cRNA probes were purified on RNAeasy mini spin columns (Qiagen) and quantified by spectrophotometer (NanoDrop Technologies, Wilmington, DE). Equal quantities of Cy3- and Cy5-labeled probes (825 μg each) were mixed and incubated in fragmentation buffer in the dark for 30 min at 60°C. After fragmentation control and respective treatment, samples were hybridized on the whole human genome (4×44 K) oligonucleotide microarrays (Agilent Technologies) for 17 h at 60°C in the dark, rotating at 10 rpm. After washing twice in GE wash buffer for 1 min, the microarray slides were washed in acetonitrile and dried. Slides were scanned by using a dual-laser microarray scanner and analyzed with Feature Extraction software (Agilent Technologies) and the Rosetta Resolver 7.2 Gene Expression Data Analysis System (Rosetta Biosoftware, Seattle, WA). All gene-array data have been submitted to www.ebi.ac.uk/arrayexpress and can be accessed through the following reviewer login: *Username: Reviewer_E-MEXP-2263 Password: 1248259780826 Password: 1248259780826.*

### *iTRAQ labeling and laser-desorption–matrix-assisted laser desorption ionization mass spectrometry*

Ferrous Hb was incubated with different GOX concentrations (1.2, 5, and 10 mU/ml) in cell-culture medium containing 4 mg/ml glucose and 5% FCS for 8 h. A total of 30 μg protein of each sample was dried in a speed vacuum concentrator for 3 h and resuspended with 20 μl of dissolution buffer (0.5 *M* triethylammonium bicarbonate and 0.05% SDS), reduced, and alkylated as described in the iTRAQ protocol (Applied Biosystems, Inc., Foster City, CA). Each sample was digested with 1 mg/ml trypsin (Promega, Madison, WI) at a trypsin-to-protein ratio of 1:10 at 37°C overnight and labeled with the iTRAQ reagent, as described in the manufacturer's manual (Applied Biosystems). The proteins from the control condition were labeled with iTRAQ reagent 114, and oxidized conditions, with 115, 116, and 117, respectively. The labeled samples were pooled and purified by using a cation-exchange cartridge (ICAT; Applied Biosystems). The bound peptides were collected with 10 m*M* $KH_2PO_4$, 350 m*M* KCl, 25% ACN. The labeled samples were dried in a vacuum concentrator. Dried peptides were redissolved in 20 μl of 2% (vol/vol) acetonitrile/0.1% trifluoroacetic acid, automatically injected by a Famos autosampler and separated by an UltiMate capillary LC system (Dionex - LC Packings) by using a 75-μm ID reverse-phase column.

**Nano-LC separation and MALDI target spotting of tryptic peptides.** Peptide separation was performed on an Ultimate chromatography system (Dionex-LC Packings, Sunnyvale, CA) equipped with a Probot MALDI spotting device. Five microliters of the samples was injected by using a Famos autosampler (Dionex-LC Packings) and loaded directly onto a 75 μm×150 mm reversed-phase column (PepMap 100, 3 μm; Dionex-LC Packings). Peptides were eluted at a flow rate of 300 nl/min by using the following gradient: 0–10 min, no solvent B; 10–105 min, none to 50% solvent B; and 105–115 min, 50 to 100% solvent B. Solvent A contained 0.1% TFA

in 95:5 water/acetonitrile, and solvent B contained 0.1% TFA in 20:80 water/acetonitrile. For MALDI analysis, the column effluent was directly mixed with MALDI matrix (3 mg/m; α-cyano-4-hydroxycinnamic acid in 70% acetonitrile/0.1% TFA) at a flow rate of 1.1 μl/min via a μ-Tee fitting. Fractions were automatically deposited every 10 s onto a MALDI target plate (Applied Biosystems/MDS Sciex, Foster City, CA) by using a Probot microfraction collector. In total, 416 spots were collected from each HPLC run.

MALDI-TOF/TOF mass spectrometry. MALDI plates were analyzed on a 4800 MALDI TOF/TOF system (Applied Biosystems) equipped with an Nd:YAG laser operating at 200 Hz. All mass spectra were recorded in positive reflector mode and generated by accumulating data from 600 laser shots. First, MS spectra were recorded from peptide standards on each of the six calibration spots, and the default calibration parameters were updated. Second, MS spectra were recorded for all sample spots on the MALDI target plate (416 spots per sample, four samples per plate). The MS spectra were recalibrated internally based on the ion signal of neurotensin peptide (Sigma).

The following threshold criteria and settings were used for the acquisition of MS/MS spectra: mass range, 800 to 4,000 Da; minimum signal-to-noise (S/N) for MS/MS acquisition, 100; maximum number of peaks/spot, eight. Peptide CID was performed at a collision energy of 1 kV and a collision gas pressure of approximately $2.5\times10^{-6}$ Torr. During MS/MS data acquisition, a method with a stop condition was used. In this method, a minimum of 1,000 shots (20 subspectra accumulated from 50 laser shots each) and a maximum of 2,000 shots (40 subspectra) were allowed for each spectrum. The accumulation of additional laser shots was halted whenever at least six ion signals with an S/N of at least 60 were present in the accumulated MS/MS spectrum, in the region above m/z 200.

Peptide and protein identification and quantification by database searching. MS/MS data analysis was performed by using ProteinPilot 2.0.1 software (Applied Biosystems) with the Paragon algorithm as the default search program. Trypsin was selected as the digestion agent, and 4-plex iTRAQ labeling and MMTS modification of cysteine were specified.

### *Scanning electron microscopy*

Cells were cultured on round (12-mm) coverslips. After treatment with GOX (5 mU) and Hb (1 mg/ml) for 8 h, cells were washed and fixed with 2% glutaraldehyde in PBS. The fixed cells were washed and postfixed in 1% $OsO_4$, dehydrated by successive immersions in increasing concentrations of ethanol, followed by CPD (critical point drying, BaL-TEC CPD 030). The dried coverslips with the dehydrated cells were mounted on SEM carbon stubs and coated with platin (5 nm). Pictures were taken at 2 kV with a SEM Zeiss Gemini 1530 (Zeiss, Oberkochen, Germany).

### *Statistical analysis*

Differences between treatment groups were analyzed with ANOVA and the Bonferroni posttest by using GraphPad Prism version 5.01, where applicable. A $p$ value $< 0.01$ was considered significant.

## Results

### *Reaction with Hb abolishes the accumulation of $H_2O_2$ generated by the glucose-glucose oxidase (GOX) system in cell culture*

To investigate the chemical interactions of low levels of $H_2O_2$ with extracellular Hb and their influence on cell-viability and gene-expression patterns, we established a glucose-glucose oxidase (GOX) system. This enzymatic system mimics a continuous, and thus, a more physiologic low-level $H_2O_2$ exposure than does the bolus addition of $H_2O_2$ (14). The GOX activity of 10 mU/ml in the presence of 4 mg/ml glucose was found to be reproducibly depleting GSH and significantly reducing cell viability over an incubation period of 8 h in VSMCs and in the mouse macrophage cell line RAW264.7. With the luminescent probe AcriglGlow, which emits light in the presence of $H_2O_2$, we could follow the production and accumulation of $H_2O_2$ in cell-culture medium, reaching a plateau intensity after an incubation period of 4 h (Fig. 1A). In the presence of Hb, we could not detect any signal over the whole 8-h reaction period. This indicates that either the generation of $H_2O_2$ is impaired by Hb or that the GOX-generated $H_2O_2$ is immediately consumed by the peroxidase activity of Hb. The same pattern of GOX-generated $H_2O_2$ accumulation in cell-culture supernatant and complete depletion of $H_2O_2$ by Hb could be confirmed by using an alternative assay based on AmplexRed fluorescence (Fig. 1B). The presence of Hb did not affect the performance of the $H_2O_2$ assays, as comparable results were obtained when samples were ultrafiltrated (to remove Hb) before measurements.

The reactions of Hb heme-iron with GOX-derived $H_2O_2$ were studied with spectrophotometry. Previous work by Cashon and Alayash (9) demonstrated differences in ferrous Hb and chemically cross-linked Hbs in their ability to form stable ferryl Hb. UV-visible spectrophotometry data consistent with Cashon and Alayash shows that ferrous Hb briefly engages in a pseudoperoxidase reaction in the presence of $H_2O_2$ generated by the glucose/GOX system (Fig. 1B, left). However, when starting with ferrous Hb, the peroxidase activity is lost within 50 min after the start of the reaction, and both heme and Hb become degraded in the spectra. Conversely, when ferric Hb is exposed to the same glucose/GOX system of $H_2O_2$ generating the ferric, heme spectra remains stable over >2 h of continuous $H_2O_2$ exposure (Fig. 1C right). For the starting material ferrous Hb, the concentration changes of ferric and ferryl Hb with the loss of ferrous Hb are shown in Fig. 1D, E. UV-VIS spectrophotometry revealed a time-dependent oxidation of heme iron in the presence of GOX, and therefore proves that Hb-heme reacts with the GOX-generated $H_2O_2$. Thus, the absence of $H_2O_2$ accumulation in the presence of Hb is not a result of suppressed enzymatic activity or the decomposition of $H_2O_2$ by possible Hb contaminants such as superoxide dismutase and catalase. Instead, GOX-generated $H_2O_2$ is consumed by Hb. Importantly, in all these studies, we used a highly purified and extensively characterized Hb preparation that has been proven to contain no RBC superoxide dismutase or catalase contamination.

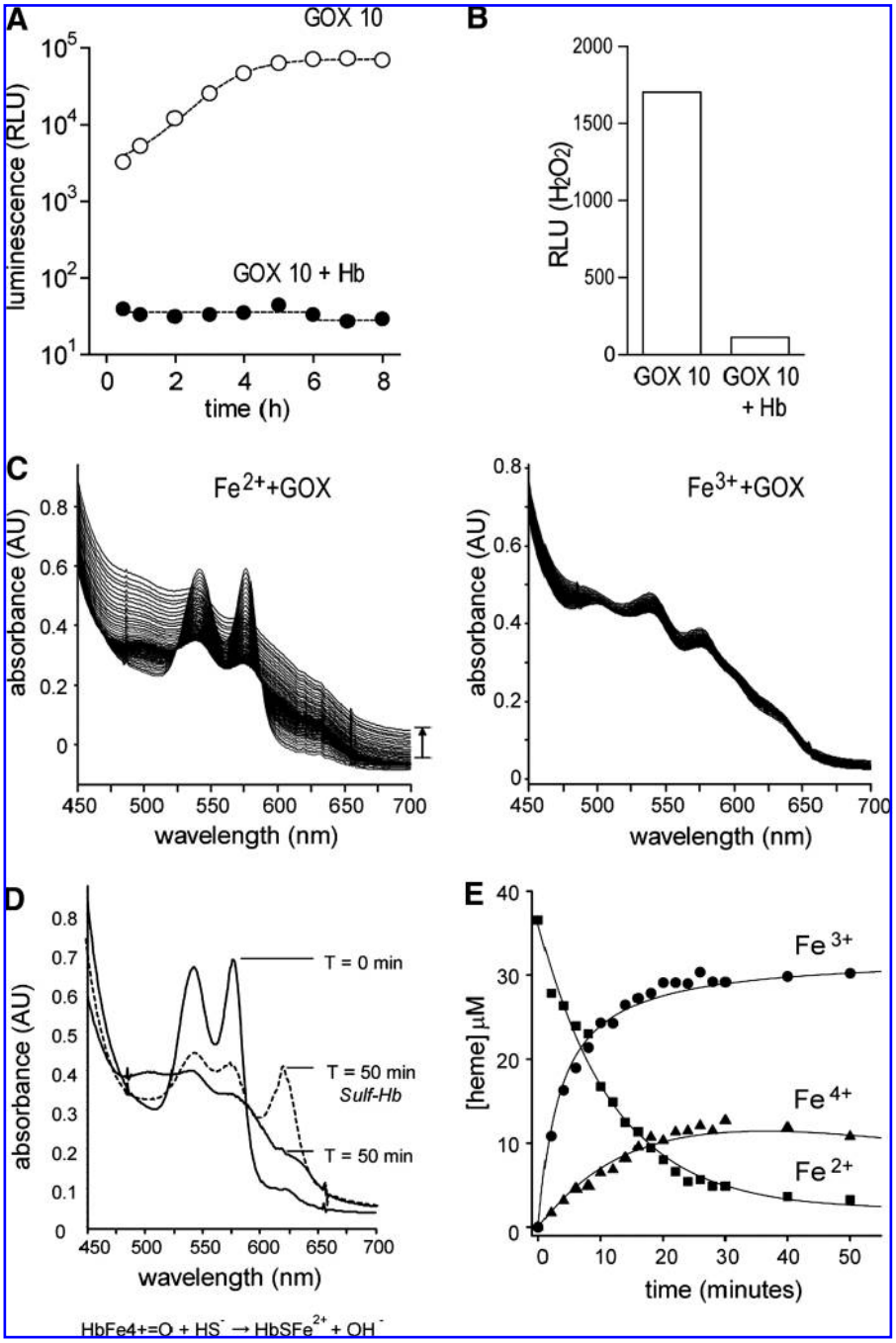


**FIG. 1. Heme redox-cycle and consumption of GOX-derived $H_2O_2$ by Hb.** (**A**) $H_2O_2$ accumulation in the cell-culture medium resulting from an active glucose-GOX system (4 mg/ml glucose, 10 mU/ml GOX) was intermittently measured with the $H_2O_2$-induced luminescence of AcriGlow (first measurement, ~15 min after the start of reaction). No $H_2O_2$ could be detected when Hb at 1 mg/ml was added at the beginning of the reaction (*black dots*). (**B**) Alternatively, $H_2O_2$ generated by GOX was measured in VSMC cell-culture supernatants with the Amplex Ultra Red assay after incubation with or without Hb for 8 h. Ultrafiltration at the end of the incubation/reaction period to remove Hb from the sample medium did not change assay results. (**C**) Damaged hemoglobin is observed in the 500- and 700-nm regions of the UV-visible spectra when the starting material is ferrous Hb (*left*) compared with ferric Hb (*right*). In culture media with fetal calf serum, spectra were obtained every 2 min over a 2-h period and demonstrated a gradual increase in absorbance at these wavelengths, starting at 50 min after the addition of GOX to ferrous Hb. Conversely, ferric Hb remained stable in the $HbFe^{3+}$ form over a 2-h period. (**D**) Addition of 2 m*M* sodium sulfide ($Na_2S$) generates the spectra for sulf-Hb (a measure of ferryl Hb; *dotted line*). (**E**) The time course of ferrous ($Fe^{2+}$), ferric ($Fe^{3+}$), and ferryl ($Fe^{4+}$) Hb is shown before Hb damage and determined as described in Materials and Methods. In all panels, data from one representative experiment are shown.

### *Screening of cell spreading and cell viability by impedance measurement suggests a protective role of ferrous and ferric Hb against $H_2O_2$-mediated oxidative cell damage*

We measured cell monolayer impedance of HEK293 cells as a function of time in the presence of different concentrations of glucose oxidase and with or without 3 mg/ml of either ferrous or ferric Hb. The xCELLigence system used in these studies provides a cell index (CI) that increases as a function of cell attachment, spreading, and cell growth, and, conversely, declines as a function of cell detachment and cell death. In Fig. 2A, the homogeneous attachment and spreading of HEK293 cells in culture (in a 96-well plate) is shown. Figure 2B illustrates the cellular (CI) response to different GOX-generated $H_2O_2$ levels. Different concentrations of GOX with and without Hb ($Fe^{2+}$ or $Fe^{3+}$) were added to the cell culture 4 h after seeding (indicated by the black arrows). A dose- and time-dependent decrease in CI could be observed with GOX in the absence of Hb. The drastic decline in CI observed with 10 mU/ml and 5 mU/ml of GOX was associated with visible rounding of the cells and detachment after >20 h of incubation. In contrast, the still significant but slighter changes in CI observed at 2.5 mU/ml GOX that

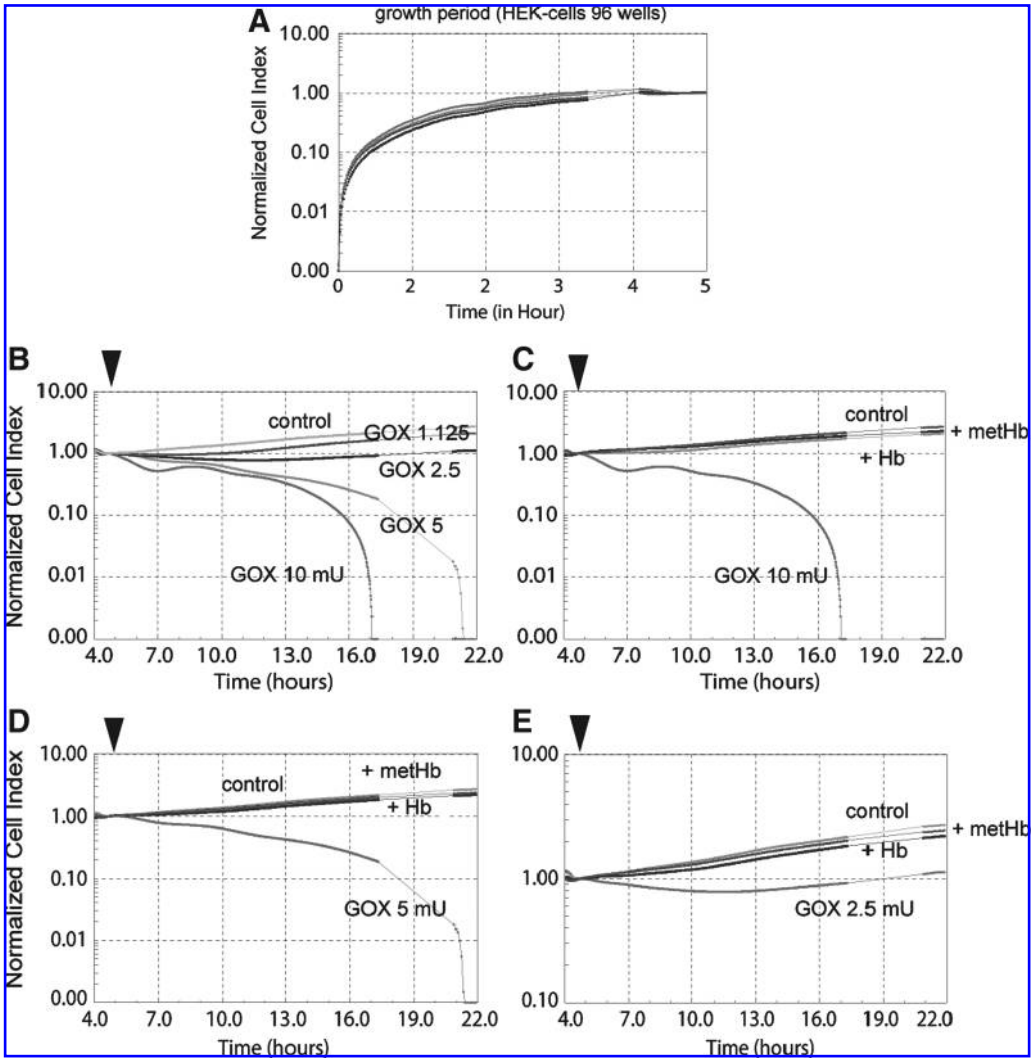


**FIG. 2. On-line cell-culture impedance measurement: cell spreading, growth, and $H_2O_2$ toxicity.** Impedance was measured on-line in cell culture by using the CELLigence RTCP-SP system. HEK293 cells were seeded at time 0 min, and the cell index, which is a function of adherence, spreading, and cell growth, was measured every 5 min (**A**). After 4 h, growth medium was replaced with serum-free medium containing the indicated concentrations of glucose oxidase (GOX) with or without Hb (as $Fe^{2+}$ or $Fe^{3+}$). The cells were kept in culture for another 18 h (**B–E**). The decline of the cell index observed in the presence of the higher GOX concentrations was associated with extensive rounding of the cells, subsequent detachment from the cell-culture surface, and cell death. No morphologic changes were observed in the presence of Hb. Individual data points represent the mean of independent values from eight wells acquired every 5 min. (For interpretation of the references to color in this figure legend, the reader is referred to the web version of this article at www.liebertonline.com/ars).

produce steady-state $H_2O_2$ concentrations far less than 10 $\mu M$ did not result in visible changes in cell morphology. Cell-impedance measurement thus proved to be a sensitive method to detect $H_2O_2$-induced cellular responses in real time. As shown in Fig. 2C–E, ferrous and ferric Hb completely prevented the $H_2O_2$-induced changes in CI. Similar experiments were performed with incubation times and on-line monitoring of up to 40 h. No difference between control and GOX + Hb samples could be detected at any time-point and $H_2O_2$-exposure level tested.

After having demonstrated that both ferric and ferrous Hb can protect against $H_2O_2$-mediated cell damage, we performed the following studies with ferrous Hb, because we considered exposure to ferrous or mixed ferrous/ferric Hb a more physiologic condition than exposure to exclusively ferric Hb.

### *Decomposition by ferrous Hb prevents cellular GSH depletion and cell death during $H_2O_2$-mediated oxidative stress*

The oxidative stress exerted by $H_2O_2$ exposure depletes cellular antioxidant systems, such as reduced GSH, and eventually induces cell death by apoptosis or necrosis. To confirm and interpret the real-time results obtained with impedance measurement, we measured intracellular GSH and ATP as quantitative markers of cellular antioxidant capacity and cell viability, respectively, in the absence and in the presence of different concentrations of GOX. We also examined different and physiologically more relevant cell types (macrophages and vascular smooth muscle cells) than in the screening experiments. After 8 h, we found a dose-dependent depletion of GSH and ATP, which resulted in an almost 100%

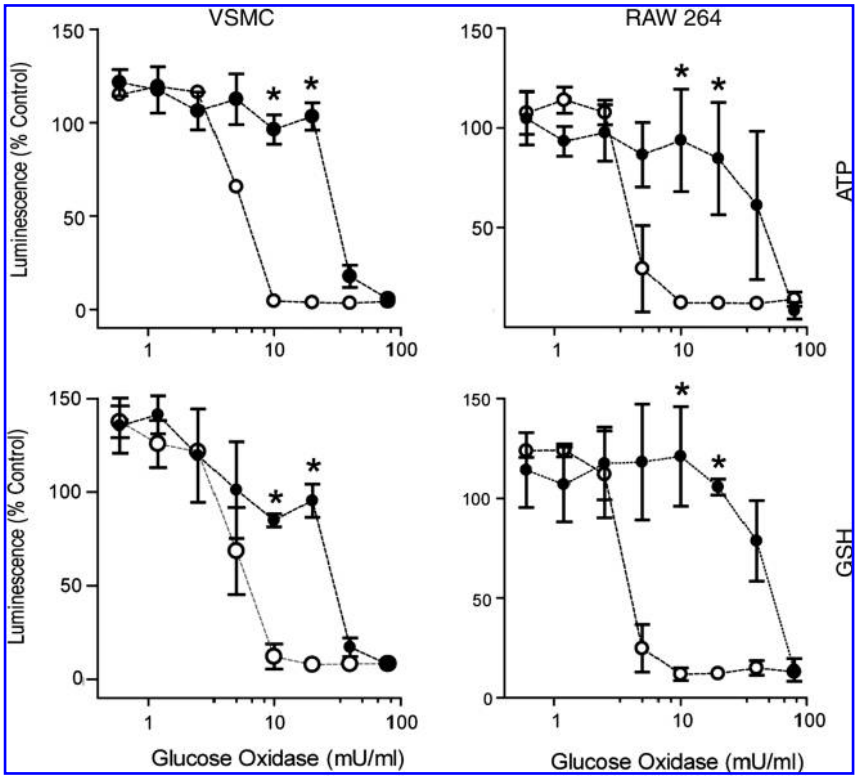


**FIG. 3. Hb prevents glutathione and ATP depletion in vascular smooth muscle cells and macrophage-like cells exposed to GOX-generated $H_2O_2$.** Intracellular-reduced glutathione (GSH) and ATP levels were measured as surrogate markers for cellular antioxidant capacity and viability, respectively, after 8 h of exposure to $H_2O_2$ generated by different GOX concentrations/activities (1.2–80 mU/ml). In the presence of Hb (1 mg/ml, red dots), the GOX activity-dependent decline curves for GSH and ATP are significantly shifted toward the right, indicating a protective effect of Hb on cellular redox status and viability. Luminescence is shown relative to that of nontreated cells. Data represent mean ± SD of at least three independent experiments. Differences of treatment groups were statistically analyzed with ANOVA for GOX, 10 mU/ml, and GOX, 20 mU/ml, and were found to be significantly different (*$p < 0.001$).

loss of GSH and ATP at concentrations of more than 5 mU/ml GOX (Fig. 3). This observation was compatible with the light-microscopy observation of extensive cell detachment after >12-h exposure to GOX activities above 10 mU/ml. Both intracellular GSH and ATP levels were maintained at baseline levels up to GOX activities of 20 mU/ml when Hb, at a concentration of 1 mg/ml, was added to the cell culture. After establishing that Hb can prevent $H_2O_2$-induced GSH and intracellular ATP depletion, we aimed to confirm on a transcriptional level that Hb also can prevent the cellular transcriptional stress response induced on $H_2O_2$ exposure.

### *Hb blunts the $H_2O_2$-driven oxidative stress transcriptional response in vascular smooth muscle cells*

To assess the global transcriptional response to $H_2O_2$ exposure generated by the GOX system, we have compared the RNA expression profile of VSMCs exposed to 5 mU/ml of GOX for 8 h in the absence or presence of 1 mg/ml Hb. The activity of 5 mU/ml of GOX was reproducibly associated with a measurable reduction in cellular GSH and ATP levels, but did not result in visible cytotoxicity within the 8-h incubation period. The global gene-expression pattern induced by GOX ± Hb, as assessed by the relative abundance of >19,000 Unigene clusters, represented on the Agilent human whole-genome arrays is shown in Fig. 4. In this representation of the transcriptome data, it becomes evident that the $H_2O_2$ exposure induces a vivid change of gene expression with many up- or downregulated genes, as indicated by the wide spreading of gene data points along the (log) ratio axis (y-axis in Fig. 4), which indicates the ratio of RNA abundance of treated compared with untreated VSMCs. Compatible with the previously described consumption of GOX-generated $H_2O_2$ by Hb, the spread of gene-expression data is significantly reduced when Hb is present in the system. In GOX-treated cells, we found 2,157 genes upregulated and 2,386 genes significantly ($p < 0.01$) downregulated. Of these, 711 were regulated more than threefold. In contrast, in the cells coincubated with GOX and Hb, we found only 1,530 and 969 genes significantly up- or downregulated, respectively, with only 108 genes regulated at a ratio above threefold (Fig. 5A). The influence of Hb on individual gene-expression levels is illustrated in Fig. 5B, in which the pairwise representation of highly $H_2O_2$-induced transcripts in the presence and absence of Hb highlights the activity of Hb to suppress $H_2O_2$-driven gene expression. High ratios of gene induction by GOX-generated $H_2O_2$ were observed for activating transcription factor 3 (ATF3) and growth-differentiation factor 15 (GDF15). ATF3 is a well-characterized oxidative stress response transcription factor; GDF15 is a stress-inducible member of the transforming growth factor superfamily. We confirmed by quantitative RT-PCR that ATF3 and GDF15 are highly induced by GOX-generated $H_2O_2$ and that this oxidative stress response is completely suppressed when Hb (1 mg/ml) is added to 10 mU/ml of GOX (Fig. 6). That $H_2O_2$ is involved in the GOX-driven alteration in gene expression in our experiments is confirmed by the fact that catalase also completely abrogates the GOX-induced ATF3 response (Fig. 6B). A similar differential gene-expression response was found for the inflammation-associated transcripts CXCL-4 and COX2. Although Hb generally reduces $H_2O_2$-stimulated alteration in gene expression in our cell-culture system, the reaction of $H_2O_2$ with Hb enhances the $H_2O_2$-induced expression of the antioxidant heme-breakdown enzyme heme oxygenase (HO-1). This response is likely to be mediated by enhanced heme

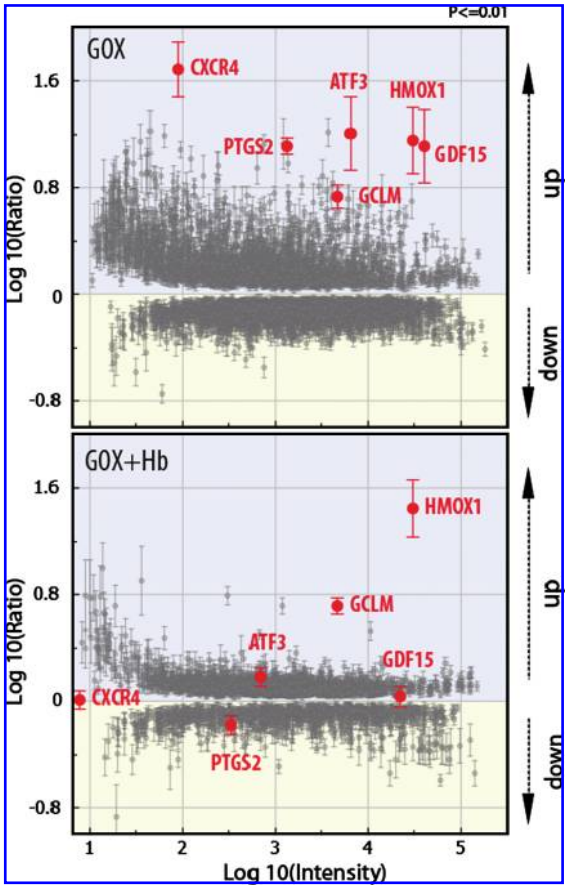


**FIG. 4. Oligonucleotide gene-array analysis of vascular smooth muscle cell gene expression evoked by GOX-generated $H_2O_2$ in the absence or presence of Hb.** Human VSMCs were exposed to the weakly cytotoxic activity of GOX (5 mU/ml) in the absence (*upper panel*) or in the presence (*lower panel*) of 1 mg/ml Hb for 8 h. The global transcriptome profile of three independent experiments was then determined with competitive hybridization gene-array analysis (Agilent human whole genome 4×44 K arrays). Each numeric result of an individual data point represents the ratio of the expression level of one gene in treated cells *versus* nontreated (control) cells. The expression levels of different sequences on the array that represent the same Unigene cluster were combined by using the Rosetta Resolver in-built error algorithm to combine experimental data on a Unigene level. Each dot represents the mean (±error of three experiments) of the expression ratio of one individual Unigene cluster (gene). Only genes with an mRNA expression ratio significantly different from 1 ($p < 0.01$) are shown. Upregulated genes (log ratio >0) are within the blue area, and downregulated genes (log ratio <0) are within the yellow area of the plot. The X-axis represents the hybridization signal intensity that is roughly proportional to the baseline mRNA abundance. (The gene symbols highlighted in red are *ATF3*, activating transcription factor 3; *GDF15*, growth-differentiation factor 15; *HMOX*, heme oxygenase 1; *GCLM*, glutamate-cysteine ligase modifier subunit; *CXCR4*, chemokine (CXC motif) receptor 4; *PTGS2*, prostaglandin-endoperoxide synthase 2 (COX2). For exact fold changes and *p* values of individual genes, see Table 1. (For interpretation of the references to color in this figure legend, the reader is referred to the web version of this article at www.liebertonline.com/ars).

release from oxidized Hb (Fig. 6D). The latter hypothesis is supported by the observation that when heme release from methemoglobin is inhibited by the addition of stoichiometric concentrations of the Hb-binding plasma protein, haptoglobin (Hp), the superinduction of HO-1 can be suppressed (data not shown). We recently showed that complex formation with Hp does not alter the ability of Hb to redox cycle $H_2O_2$ (7).

### *Extensive Hb amino acid oxidation and precipitation suggests that globin acts as a scavenger for heme-generated radicals in the presence of GOX-generated $H_2O_2$*

Under highly controlled reaction conditions (*i.e.*, bolus addition of a 10-fold molar concentration of $H_2O_2$ to Hb in the absence of small molecular reductants or other proteins or both), the reaction of $H_2O_2$ with Hb results in a reproducible pattern of $\beta$-globin chain amino acid oxidations and $\alpha$-globin chain polymerization. Primary oxidized amino acids within the Hb $\beta$-chain are Cys93, Trp15, and Cs112. These cross-linking and amino acid oxidation reactions are supposed to be driven by the radicals generated in the reaction of Hb-heme with $H_2O_2$. Therefore, the protective activity of Hb against $H_2O_2$-induced oxidative stress in our cell-culture systems could be a combined result of $H_2O_2$ removal by heme redox cycling and subsequent scavenging of toxic radicals within Hb cross-links and globin amino acid oxidations. To find the structural evidence of these events, we applied a quantitative mass-spectrometry method on the basis of isobaric tag peptide labeling (iTRAQ) in combination with MALDI-TOF-MS/MS to measure the extent of GOX-driven oxidation of $\beta$Cys93. As shown in Fig. 7, the presence of GOX at 5 or 10 mU/ml shifts the ratio of oxidized to nonoxidized cysteine toward a >20-fold excess of triply oxidized cysteic acid over the nonoxidized globin after an 8-h incubation period. In addition, the $H_2O_2$ reaction with Hb in our cell-culture conditions results in a dense precipitate. This precipitate, which did not occur at all when cells were incubated with any concentration of only Hb or GOX, probably corresponds to the heme-adducted globin polymers, which we previously characterized by high-mass MALDI MS (Fig. 8).

## Discussion

The radicals emanating from Hb when it reacts with oxidants have been proposed to be a primary source of Hb-derived toxicity (8, 10). Conversely, the reaction of Hb with hydrogen peroxide can potentially remove the potentially toxic oxidant from peroxidative environments. Multiple kinetic and environmental factors might therefore determine the net biologic effect of radical generation and $H_2O_2$ removal by Hb during oxidative-stress conditions. In this study, we showed that ferrous and ferric Hb can protect various cell types against the cytotoxicity that normally results from the continuous low-level $H_2O_2$ exposure generated by an enzymatic system. Additionally, the transcriptional stress response exerted by this low-level $H_2O_2$ exposure was effectively suppressed by Hb, thus supporting a true antioxidant potential of Hb. The rationale used to explain the $H_2O_2$ consumption and associated cellular protection observed in our systems is demonstrated in the UV-visible spectra, where ferrous and ferric Hb are shown to redox cycle $H_2O_2$ generated by the GOX enzymatic system in cell-culture conditions.

Table 1. Transcripts More Than Fivefold Induced by GOX Treatment of VSMCs for 8 h and Corresponding Data for GOX Treatment in the Presence of Ferrous Hb

| | | | *GOX* (n = 3) | | *GOX + Hb* (n = 3) | |
|---|---|---|---|---|---|---|
| *UniGene code* | | *Description* | *Fold change* | p *Value* | *Fold change* | p *Value* |
| **Hs.421986** | **CXCR4** | **Chemokine (C-X-C motif) receptor 4** | **47.638** | **1.14E-22** | **1.005** | **0.937** |
| Hs.530749 | PPFIA4 | Protein tyrosine phosphatase | 16.277 | 2.40E-17 | 1 | 1 |
| Hs.9613 | ANGPTL4 | Angiopoietin-like 4 | 16.062 | 2.29E-40 | −1.267 | 0.002 |
| **Hs.460** | **ATF3** | **Activating transcription factor 3** | **15.84** | **5.79E-07** | **1.477** | **5.4E-08** |
| **Hs.517581** | **HMOX1** | **Heme oxygenase (decycling) 1** | **14.042** | **4.28E-08** | **27.373** | **1.4E-15** |
| Hs.47357 | CH25H | Cholesterol 25-hydroxylase | 13.587 | 5.15E-22 | 1.052 | 0.888 |
| Hs.530443 | LOC387763 | Hypothetical LOC387763 | 13.176 | 2.18E-10 | 1.052 | 0.689 |
| Hs.25647 | FOS | V-fos FBJ murine osteosarcoma viral | 13.138 | 0 | 1.023 | 0.7 |
| **Hs.196384** | **PTGS2** | **Prostaglandin-endoperoxide synthase** | **12.637** | **0** | **−1.536** | **4.3E-12** |
| **Hs.515258** | **GDF15** | **Growth-differentiation factor 15** | **12.561** | **2.82E-06** | **1.061** | **0.457** |
| Hs.172130 | ZP1 | Zona pellucida glycoprotein 1 | 12.005 | 0 | −2.028 | 0.241 |
| Hs.159523 | CRTAM | Class-I MHC-restricted T-cell associated | 11.483 | 0 | 1 | 1 |
| Hs.268490 | NR0B1 | Nuclear receptor subfamily 0, group B | 11.046 | 5.75E-21 | 2.438 | 2.5E-05 |
| Hs.413297 | RGS16 | Regulator of G-protein signaling 16 | 10.196 | 2.46E-32 | −1.197 | 0.176 |
| Hs.9730 | TAC3 | Tachykinin 3 (neuromedin K, neurokinin | 9.812 | 2.63E-24 | 1 | 1 |
| Hs.390594 | SLC7A11 | Solute carrier family 7, member 11 | 9.453 | 0 | 5.098 | 0 |
| Hs.492490 | PVRL4 | Poliovirus receptor related 4 | 9.452 | 4.93E-08 | 1 | 1 |
| Hs.83465 | HOXD1 | Homeobox D1 | 9.206 | 8.13E-22 | 1.298 | 0.56 |
| Hs.642679 | MAFB | V-maf musculoaponeurotic fibrosarcoma | 9.107 | 2.57E-24 | −1.03 | 0.766 |
| Hs.611485 | Hs.611485 | *Homo sapiens*, clone IMAGE:2960704 | 8.04 | 4.24E-08 | 1.749 | 0.098 |
| Hs.583896 | C8orf12 | L-threonine dehydrogenase | 7.97 | 1.08E-10 | 1 | 1 |
| Hs.390221 | TEX14 | Testis-expressed sequence 14 | 7.914 | 1.61E-11 | 1.065 | 0.722 |
| Hs.288998 | S100A14 | S100 calcium-binding protein A14 | 7.868 | 9.53E-13 | −1.124 | 0.808 |
| Hs.534313 | EGR3 | Early growth response 3 | 7.639 | 3.69E-11 | 1 | 1 |
| Hs.96 | PMAIP1 | Phorbol-12-myristate-13-acetate induced | 7.582 | 7.07E-16 | 1.253 | 1.8E-04 |
| Hs.631555 | DHDH | Dihydrodiol dehydrogenase (dimeric) | 7.581 | 0 | −1.115 | 0.586 |
| Hs.592601 | AK3L1 | Adenylate kinase 3–like 1 | 7.567 | 3.04E-10 | 1.217 | 0.167 |
| Hs.17958 | GAL3ST1 | Galactose-3-*O*-sulfotransferase 1 | 7.364 | 1.78E-29 | 2.8 | 1.6E-04 |
| Hs.584876 | FLRT1 | Fibronectin leucine-rich transmembrane | 7.021 | 7.66E-07 | 1.127 | 0.767 |
| Hs.150595 | CYP26A1 | Cytochrome P450, family 26, subfamily A | 6.957 | 6.19E-09 | −1.007 | 0.985 |
| Hs.264606 | Hs.264606 | Full-length insert cDNA clone ZD68B12 | 6.955 | 4.52E-21 | 1.27 | 0.328 |
| Hs.181297 | LOC283666 | Hypothetical protein LOC283666 | 6.944 | 2.26E-05 | 1.094 | 0.294 |
| Hs.632832 | RAB39B | RAB39B, member RAS oncogene family | 6.83 | 1.45E-14 | −1.082 | 0.577 |
| Hs.48029 | SNAI1 | Snail homologue 1 (*Drosophila*) | 6.676 | 4.66E-29 | 1.103 | 0.237 |
| Hs.594689 | Hs.594689 | Full-length insert cDNA clone ZE05E03 | 6.661 | 3.76E-16 | 2.65 | 0.002 |
| Hs.519162 | BTG2 | BTG family, member 2 | 6.42 | 0 | −1.058 | 0.429 |
| Hs.349204 | SOST | Sclerosteosis | 6.418 | 7.90E-08 | 1 | 1 |
| Hs.231897 | FLJ35767 | FLJ35767 protein | 6.391 | 1.82E-14 | 2.076 | 0.024 |
| Hs.132701 | CCDC11 | Coiled-coil domain containing 11 | 6.379 | 3.45E-08 | 2.156 | 0.228 |
| Hs.1027 | RRAD | Ras-related associated with diabetes | 6.326 | 0 | −1.096 | 0.097 |
| Hs.420244 | FAM80A | Family with sequence similarity 80 | 6.275 | 6.61E-20 | 1.132 | 0.756 |
| Hs.2233 | CSF3 | Colony-stimulating factor 3 (granulocyte) | 6.272 | 0 | −1.485 | 0.215 |
| Hs.563344 | NR4A2 | Nuclear-receptor subfamily 4, group A | 6.259 | 7.10E-14 | 1.221 | 0.354 |
| Hs.469663 | ZSCAN4 | Zinc-finger and SCAN domain–containing 4 | 6.239 | 3.02E-25 | 1.525 | 0.322 |
| Hs.636352 | Hs.636352 | CDNA: FLJ23572 fis, clone LNG12403 | 6.076 | 7.94E-05 | −1.018 | 0.958 |
| Hs.444947 | TRIB1 | Tribbles homologue 1 (*Drosophila*) | 6.009 | 4.14E-29 | 1.324 | 0.02 |
| Hs.539969 | ARHGAP9 | Rho GTPase–activating protein 9 | 5.839 | 1.05E-10 | −1.063 | 0.849 |
| Hs.437126 | SPATA4 | Spermatogenesis-associated 4 | 5.832 | 0 | 1.085 | 0.644 |
| Hs.481235 | ACTA1 | Actin, alpha 1, skeletal muscle | 5.759 | 3.54E-14 | 2.08 | 0.155 |
| Hs.1288 | ARC | Activity-regulated cytoskeleton-associated | 5.646 | 0 | −1.198 | 0.324 |
| Hs.40888 | AOC3 | Amine oxidase, copper-containing 3 | 5.603 | 1.45E-07 | 1.312 | 0.026 |
| Hs.198241 | JMJD1A | Jumonji domain–containing 1A | 5.57 | 0 | 1.359 | 1.0E-06 |
| Hs.557425 | GDF9 | Growth-differentiation factor 9 | 5.565 | 3.06E-22 | −1.056 | 0.895 |
| Hs.25022 | RASL11B | RAS-like, family 11, member B | 5.45 | 2.08E-14 | −1.306 | 0.067 |
| Hs.8035 | AREG | Amphiregulin | 5.42 | 1.80E-42 | 1.634 | 0.001 |
| **Hs.270833** | **GCLM** | **Glutamate-cysteine ligase** | **5.288** | **0** | **5.104** | **0** |
| Hs.315562 | GRHL3 | Grainyhead-like 3 (*Drosophila*) | 5.263 | 5.09E-19 | 1.207 | 0.609 |
| Hs.369825 | TRIM73 | Tripartite motif–containing 73 | 5.214 | 7.66E-15 | 1.546 | 0.106 |
| Hs.632307 | FOSB | FBJ murine osteosarcoma viral oncogene | 5.165 | 0 | 1.255 | 0.109 |
| Hs.590958 | CXCL3 | Chemokine (C-X-C motif) ligand 3 | 5.151 | 9.40E-22 | −1.124 | 0.026 |
| Hs.89690 | FLJ26850 | FLJ26850 protein | 5.083 | 2.21E-09 | 1.251 | 0.646 |
| Hs.628968 | SPANXB2 | SPANX family, member B2 | 5.069 | 5.55E-06 | −1.104 | 0.368 |
| Hs.643547 | HK2 | Hexokinase 2 | 5.056 | 4.13E-15 | 1.029 | 0.741 |
| Hs.591588 | Hs.437039 | CDNA clone IMAGE:5288757 | 5.05 | 3.04E-05 | 1.813 | 0.242 |
| Hs.437039 | LOC644242 | Hypothetical protein LOC644242 | 5.028 | 2.31E-08 | 1.647 | 0.372 |
| Hs.515383 | MGC42105 | Hypothetical protein MGC42105 | 5.003 | 2.03E-32 | −1.136 | 0.453 |

Genes in boldface are highlighted in Fig. 3.

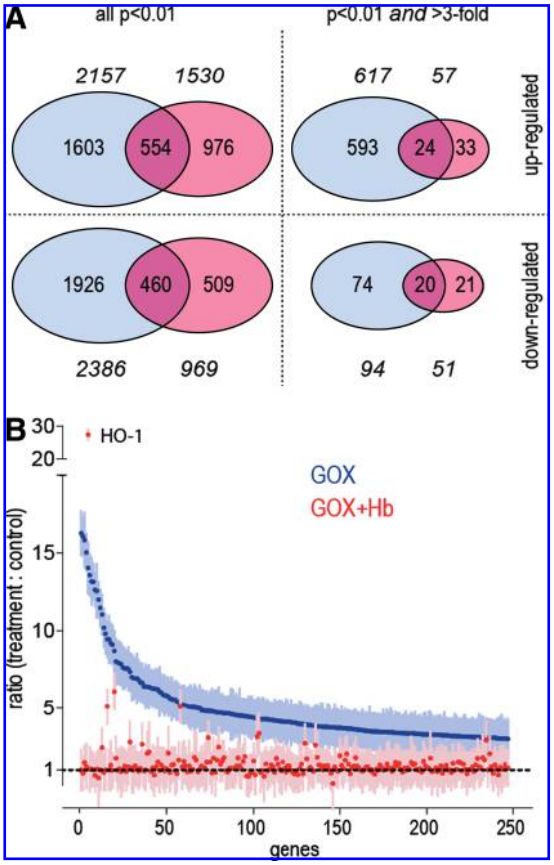


**FIG. 5. Summary of transcript regulations found with gene-array analysis of GOX-driven gene expression in the absence or presence of Hb.** (**A**) The Venn diagrams represent total numbers of transcripts found to be significantly ($p < 0.01$) up- or downregulated by GOX (5 mU/ml) in the absence (blue) or presence (red) of 1 mg/ml of Hb. In the left diagrams, all significantly regulated genes are shown; in the right diagrams, only those with a fold induction/suppression of >3 are shown. (**B**) Significantly regulated genes represented according to their fold regulation found in GOX (5 mU/ml)-treated VSMCs (blue). Regulations of the same genes in the presence of GOX + Hb (1 mg/ml) are shown at the corresponding X-axis positions in red. Data represent mean ratios of treated *versus* nontreated cells of three independent experiments (±error). A ratio of 1 indicates no change in transcript abundance. For exact fold changes and *p* values of individual genes, see Table 1. (For interpretation of the references to color in this figure legend, the reader is referred to the web version of this article at www.liebertonline.com/ars).

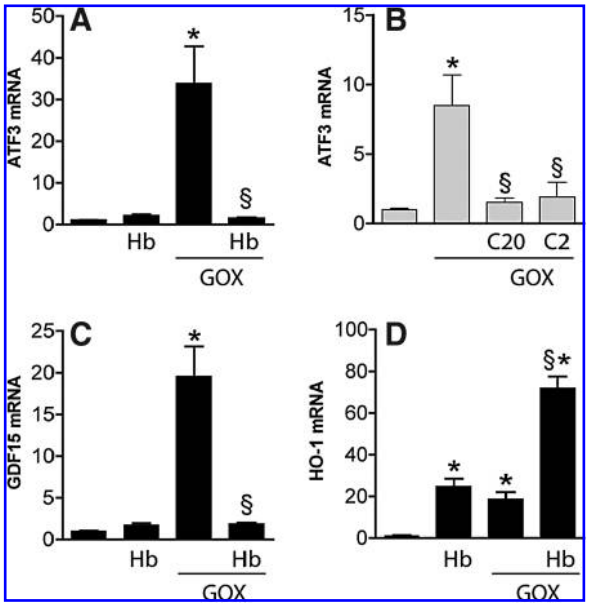


**FIG. 6. RT-PCR quantification of oxidative stress–responsive genes in VSMCs.** The mRNA abundances of oxidative stress–responsive genes were determined with quantitative RT-PCR after incubation for 8 h with GOX (5 mU/ml) in the presence or absence of 1 mg/ml Hb (**A**, **C**, **D**) or in the presence or absence of catalase at a GOX/catalase activity ratio of 1:2 (C2) or 1:20 (C20) (**B**). All mRNA levels were normalized to HPRT abundance and are expressed relative to the mRNA abundance in untreated cells. Data represent mean ± SEM of at least three independent experiments. $^{*}p < 0.01$ for differences *vs.* untreated. $^{\S}p < 0.01$ for differences in GOX *vs.* GOX + Hb or GOX *vs.* GOX + C.

As structural consequences of these reactions, we found extensive Hb $\beta$-globin amino acid oxidations and formation of altered heme-protein products observed as aggregates with electron microscopy.

Potential *in vivo* substrates found to be highly vulnerable to the redox cycling and associated radical-generating activity of Hb are lipoproteins (LDL) and fatty acids, such as arachidonic acid, that are ubiquitously present in circulation and as critical structural components of cell membranes (26, 27, 36). The oxidation of these biomolecules can result in the generation of biologically active compounds with a wide range of inflammatory and vasoactive properties. Evidence that these Hb-driven reactions do occur *in vivo* has been provided by the observation that specific oxidative-stress markers such as 4-hydroxynonenol (4-HNE)-modified proteins are highly increased in tissues when animals are exposed to large quantities of cell-free intravascular Hb (4). *In vitro*, ferric Mb and certain chemically modified Hbs were found to induce cellular oxidative toxicity (12, 13). The toxicity resulting from reaction of heme-proteins with $H_2O_2$ might be particularly important when small molecular antioxidants, such as ascorbic or uric acid, responsible for physiologically reducing oxidized heme-iron, become depleted either on massive extracellular Hb accumulation or during prolonged oxidative stress (11).

The pseudoperoxidase activity of heme globins (*i.e.*, Hb and myoglobin Mb) was recognized decades ago. Specific heme-pocket amino acid mutations that rapidly remove $H_2O_2$ generated by autoxidation have been studied (2), and it was thereby suggested that the physiologic environmental exposure of heme globins with enhanced pseudoperoxidase activity could introduce a protective function into the protein. Further work suggested that the stabilization of Hb by chemical modification could enhance the pseudoperoxidative cycling of $H_2O_2$ by heme, with detrimental consequences to endothelial cells (12). Similar *in vitro* observations were made when cultured endothelial cells were treated with ferric Mb and a constant level of $H_2O_2$ (13). In light of the potentially hazardous effects exerted by Mb- and modified Hb-derived radicals, the $H_2O_2$-degrading function of Hb has never been accounted for as an antioxidant or a protective physiologic function of Hb. It appeared likely that, also in the case of

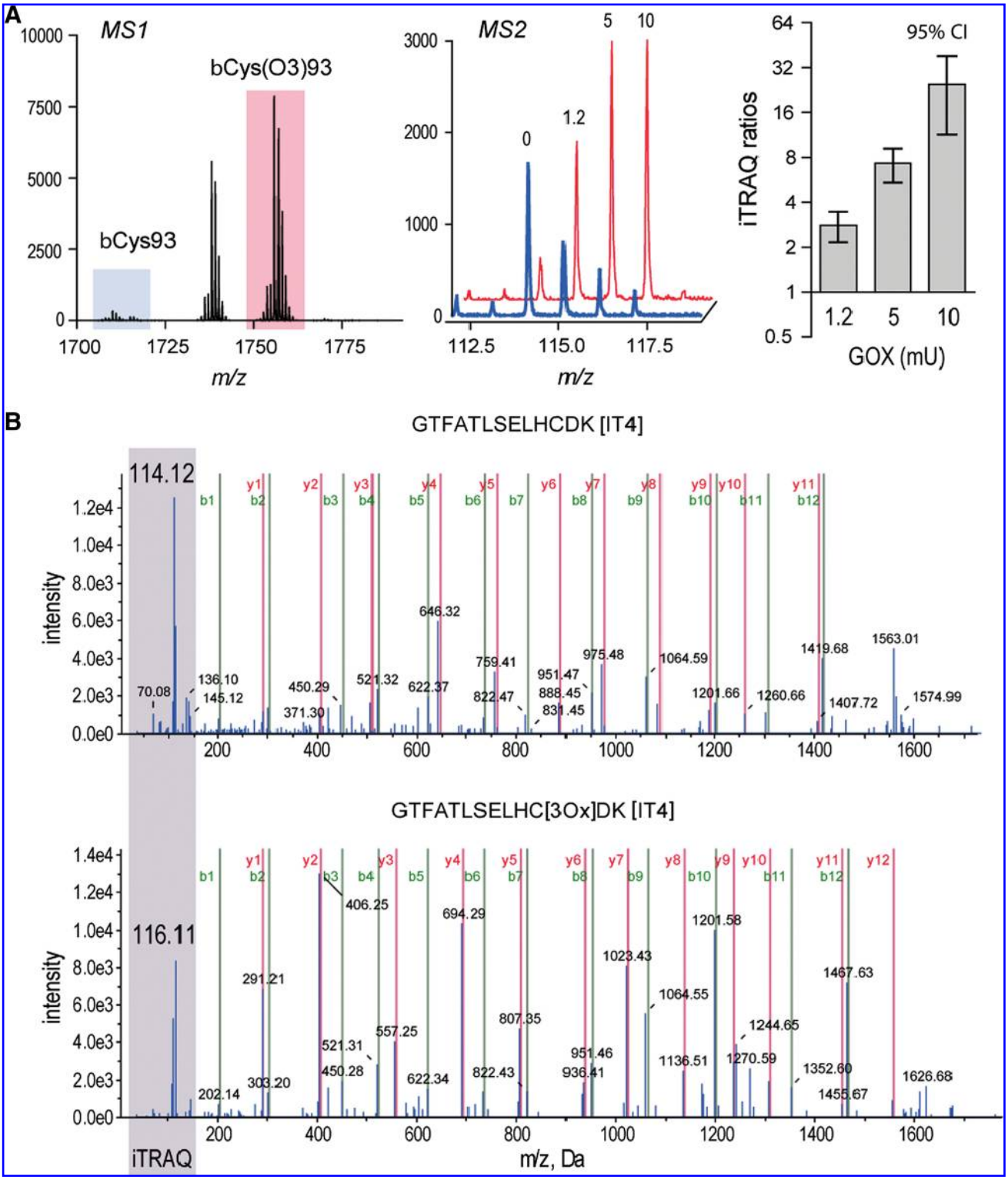


**FIG. 7. GOX activity in cell-culture medium induces extensive oxidation of *β*Cys93.** Hemoglobin incubated for 8 h with different concentrations of GOX (0–10 mU/ml) in cell-culture medium was analyzed with iTRAQ labeling and MALDI-MS/MS mass spectrometry to quantify nonoxidized and triply oxidized *β*Cys93. (**A**, *left*) Representative ion-current elution profiles of nonoxidized (blue) and oxidized *β*Cys93 in MS1. (**A**, *middle*) Representative MS2 spectra of the iTRAQ tag mass regions for nonoxidized (blue) and oxidized ($O_3$, red) *β*Cys93. Each of the four individual peaks represents the relative quantity of nonoxidized or oxidized *β*Cys93($O_3$) within one sample in the analyte mixture. The analyte mixture was composed of equal amounts of tryptic peptides from Hb treated with the different GOX concentrations, with each sample peptide tagged with a specific iTRAQ mass (114–117 m/z units). (**A**, *right*) The mean cysteic acid ($O_3$) ratio for treated (three different GOX concentrations) *versus* nontreated Hb is shown as the mean ± 95% confidence interval (CI) of three experiments. The 95% CI for all three GOX conditions does not overlap with the ratio value 1. (**B**) Fragmentation MS2 spectra of the *β*Cys93 containing tryptic peptide GTFATLSELHCDK. Nonoxidized peptide (*upper panel*). Oxidized ($O_3$) peptide (*lower panel*). (For interpretation of the references to color in this figure legend, the reader is referred to the web version of this article at www.liebertonline.com/ars).

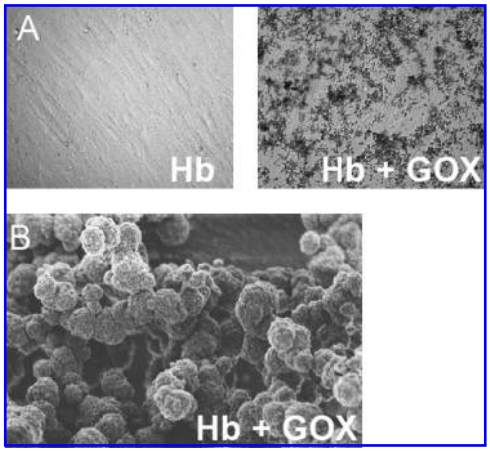


**FIG. 8. Scanning electron microscopy (SEM) image of Hb precipitate forming on VSMC cell culture on reaction of Hb with GOX-derived $H_2O_2$.** (**A**, *left*) Light microscopy image (×200 magnification) of a VSMC monolayer in the presence of 1 mg/ml Hb after 8-h incubation. (**A**, *right*) In the presence of 5 mU/ml of GOX, a dense precipitate starts to form after ~4 h of incubation. (**B**) Scanning electron microscope image of the Hb precipitate on VSMC (×40 magnification, image obtained at 2 kV).

native, nonmodified Hb, radical generation would predominate and skew the net effect of the Hb-$H_2O_2$ reactions into an oxidant and damaging biologic activity. The present study differs from previous work in that highly purified and stroma-free human Hb preparations were tested to evaluate Hb protein and cellular changes in the presence of a peroxide-generating system. Moreover, our data suggest that differences may exist among the various heme-globin peroxidase activities and their influence on cellular responses.

When Hb is reacted with $H_2O_2$ at physiologic pH, $\beta$-globin chain amino acid structural changes were observed in several studies with different techniques, including HPLC, mass spectrometry, (ESI-TOF/MS), and circular dichroism (21). The most striking modifications were amino acid oxidations within the $\beta$-globin chain, a loss of $\beta$-globin chain $\alpha$-helical structure, and decreased ellipticity in the Soret region of the CD spectrum, indicating heme loss of approximately 70% with the addition of stoichiometric concentrations of $H_2O_2$. Within the $\alpha$-globin chains, numerous heme/porphyrin Hb protein adducts and cross-links were observed (8, 21, 42).

The intriguing and complex structural changes observed when Hb is subjected to $H_2O_2$ exposure, and the evident cytoprotective activity of Hb during $H_2O_2$ exposure, support a novel protective mechanism by which Hb appears to limit cellular injury, contrary to the previously reported data when ferric Mb and certain chemically modified Hbs were evaluated (12). Certain peroxidases (mammalian and plant) exist with heme covalently bound within the active site of the peroxidase enzyme. This structural feature prevents damage to the active site by potentially reactive oxidative products of the peroxide enzymatic degradation (19, 20, 43). Therefore, it is possible that Hb uses a mechanism to protect the external cellular environment by redirecting the radical burden toward heme adduct formation, internalization of heme within the protein, heme cross-linking, or a combination of these. Likewise, a mechanism including irreversible oxidative modifications of globin amino acids could act as a sink for heme reaction–derived radicals protecting non-Hb substrates and living cells from oxidative impact. At least in the case of ferrous Hb, our spectrophotometric and EM data suggest that these cyclic reactions finally result in complete destruction of the protein.

Under the experimental conditions presented in our study, Hb can act as an antioxidant and cytoprotective peroxidase. A typical clinical situation in which large amounts of extracellular Hb could be exposed to $H_2O_2$ within an inflammation-prone tissue environment might be found in atherosclerotic plaques. Boyle *et al.* (6) recently reported the intriguing observation that macrophages confined to the regions of intraplaque hemorrhage displayed significantly less oxidative damage as compared with cells within the lipid-core area of the same plaques. Whereas an antioxidative phenotype of the macrophage itself was invoked to explain this unexpected finding, the Hb-rich environment could be an additional protective antioxidant factor.

This concept adds a novel facet to the complex biology of Hb. Our results suggest that the general view of Hb being a toxic and oxidative molecule might be too simplistic. Instead, complex interactions between the baseline oxidative state of Hb, possible structural modifications, environmental factors such as the presence of small molecular oxidants, and possibly the presence or absence of specific Hb or heme scavengers such as haptoglobin, hemopexin, or their respective cellular receptors determines the biologic impact of Hb during oxidative-stress conditions (23, 31, 38, 39, 41). It should be kept in mind that different cell types might reflect different responses to Hb or its oxidation products. For example, heme has been identified as a ligand of Toll-like receptor 4 (TLR4) and might thus induce or enhance an inflammatory response in some dedicated cell types (15). Accordingly, other pattern-recognition receptors might display specificity for heme-adducted, oxidized, or cross-linked Hb species. Considering all these factors will help to explain the role of Hb in tissue homeostasis during inflammation, tissue injury, and in hemolytic and vascular diseases.

## Acknowledgments

The study was supported by the Swiss National Science Foundation (grant 31-120658), the Gianni Rubatto Foundation, and the Helmut Horten Foundation (all to D.J.S.).

## Author Disclosure Statement

No conflict of interest has been declared by any author. The findings and conclusions in this article have not been formally disseminated by the Food and Drug Administration and should not be construed to represent any agency determination or policy.

## References

1. Alayash AI. Oxygen therapeutics: can we tame haemoglobin? *Nat Rev Drug Discov* 3: 152–159, 2004.
2. Alayash AI, Ryan BA, Eich RF, Olson JS, and Cashon RE. Reactions of sperm whale myoglobin with hydrogen peroxide: effects of distal pocket mutations on the formation and stability of the ferryl intermediate. *J Biol Chem* 274: 2029–2037, 1999.

3. Balla J, Jacob HS, Balla G, Nath K, Eaton JW, and Vercellotti GM. Endothelial-cell heme uptake from heme proteins: induction of sensitization and desensitization to oxidant damage. *Proc Natl Acad Sci U S A* 90: 9285–9289, 1993.
4. Boretti FS, Buehler PW, D'Agnillo F, Kluge K, Glaus T, Butt OI, Jia Y, Goede J, Pereira CP, Maggiorini M, Schoedon G, Alayash AI, and Schaer DJ. Sequestration of extracellular hemoglobin within a haptoglobin complex decreases its hypertensive and oxidative effects in dogs and guinea pigs. *J Clin Invest* 119: 2271–2280, 2009.
5. Boykins RA, Buehler PW, Jia Y, Venable R, and Alayash AI. *O*-raffinose crosslinked hemoglobin lacks site-specific chemistry in the central cavity: structural and functional consequences of beta93Cys modification. *Proteins* 59: 840–855, 2005.
6. Boyle JJ, Harrington HA, Piper E, Elderfield K, Stark J, Landis RC, and Haskard DO. Coronary intraplaque hemorrhage evokes a novel atheroprotective macrophage phenotype. *Am J Pathol* 174: 1097–1108, 2009.
7. Buehler PW, Abraham B, Vallelian F, Linnemayr C, Pereira CP, Cipollo JF, Jia Y, Mikolajczyk M, Boretti FS, Schoedon G, Alayash AI, and Schaer DJ. Haptoglobin preserves the CD163 hemoglobin scavenger pathway by shielding hemoglobin from peroxidative modification. *Blood* 113: 2578–2586, 2009.
8. Buehler PW and D'Agnillo F. Toxicological consequences of extracellular hemoglobin: biochemical and physiological perspectives. *Antioxid Redox Signal* 2009.
9. Cashon RE and Alayash AI. Reaction of human hemoglobin HbA0 and two cross-linked derivatives with hydrogen peroxide: differential behavior of the ferryl intermediate. *Arch Biochem Biophys* 316: 461–469, 1995.
10. Cooper CE. Radical producing and consuming reactions of hemoglobin: how can we limit toxicity? *Artif Organs* 33: 110–114, 2009.
11. Cooper CE, Silaghi-Dumitrescu R, Rukengwa M, Alayash AI, and Buehler PW. Peroxidase activity of hemoglobin towards ascorbate and urate: a synergistic protective strategy against toxicity of hemoglobin-based oxygen carriers (HBOCs). *Biochim Biophys Acta* 1784: 1415–1420, 2008.
12. D'Agnillo F and Alayash AI. Redox cycling of diaspirin cross-linked hemoglobin induces $G_2$/M arrest and apoptosis in cultured endothelial cells. *Blood* 98: 3315–3323, 2001.
13. D'Agnillo F and Alayash AI. A role for the myoglobin redox cycle in the induction of endothelial cell apoptosis. *Free Radic Biol Med* 33: 1153–1164, 2002.
14. Dhanasekaran A, Kotamraju S, Kalivendi SV, Matsunaga T, Shang T, Keszler A, Joseph J, and Kalyanaraman B. Supplementation of endothelial cells with mitochondria-targeted antioxidants inhibit peroxide-induced mitochondrial iron uptake, oxidative damage, and apoptosis. *J Biol Chem* 279: 37575–37587. 2004.
15. Figueiredo RT, Fernandez PL, Mourao-Sa DS, Porto BN, Dutra FF, Alves LS, Oliveira MF, Oliveira PL, Graca-Souza AV, and Bozza MT. Characterization of heme as activator of Toll-like receptor 4. *J Biol Chem* 282: 20221–20229, 2007.
16. Giulivi C and Davies KJ. Hydrogen peroxide-mediated ferrylhemoglobin generation in vitro and in red blood cells. *Methods Enzymol* 231: 490–496, 1994.
17. Graca-Souza AV, Arruda MAB, de Freitas MS, Barja-Fidalgo C, and Oliveira PL. Neutrophil activation by heme: implications for inflammatory processes. *Blood* 99: 4160–4165, 2002.
18. Gramaglia I, Sobolewski P, Meays D, Contreras R, Nolan JP, Frangos JA, Intaglietta M, and van der Heyde HC. Low nitric oxide bioavailability contributes to the genesis of experimental cerebral malaria. *Nat Med* 12: 1417–1422, 2006.
19. Huang L, Wojciechowski G, and Ortiz de Montellano PR. Prosthetic heme modification during halide ion oxidation: demonstration of chloride oxidation by horseradish peroxidase. *J Am Chem Soc* 127: 5345–5353, 2005.
20. Huang L, Wojciechowski G, and Ortiz de Montellano PR. Role of heme-protein covalent bonds in mammalian peroxidases: protection of the heme by a single engineered heme-protein link in horseradish peroxidase. *J Biol Chem* 281: 18983–18938, 2006.
21. Jia Y, Buehler PW, Boykins RA, Venable RM, and Alayash AI. Structural basis of peroxide-mediated changes in human hemoglobin: a novel oxidative pathway. *J Biol Chem* 282: 4894–4907, 2007.
22. Kolodgie FD, Gold HK, Burke AP, Fowler DR, Kruth HS, Weber DK, Farb A, Guerrero LJ, Hayase M, Kutys R, Narula J, Finn AV, and Virmani R. Intraplaque hemorrhage and progression of coronary atheroma. *N Engl J Med* 349: 2316–2325, 2003.
23. Levy A, Asleh R, Blum S, Levy N, Miller-Lotan R, Kalet-Litman S, Anbinder Y, Lache O, Nakhoul F, Asaf R, Farbstein D, Pollak M, Soloveichik Y, Strauss M, Alshiek J, Livshits A, Schwartz A, Awad H, Jad K, and Goldstein H. Haptoglobin: basic and clinical aspects. *Antioxid Redox Signal* 2009.
24. Liu X and Spolarics Z. Methemoglobin is a potent activator of endothelial cells by stimulating IL-6 and IL-8 production and E-selectin membrane expression. *Am J Physiol Cell Physiol* 285: C1036–C1046, 2003.
25. Locher R, Brandes RP, Vetter W, and Barton M. Native LDL induces proliferation of human vascular smooth muscle cells via redox-mediated activation of ERK 1/2 mitogen-activated protein kinases. *Hypertension* 39: 645–650, 2002.
26. Miller YI, Altamentova SM, and Shaklai N. Oxidation of low-density lipoprotein by hemoglobin stems from a heme-initiated globin radical: antioxidant role of haptoglobin. *Biochemistry* 36: 12189–12198, 1997.
27. Miller YI, Smith A, Morgan WT, and Shaklai N. Role of hemopexin in protection of low-density lipoprotein against hemoglobin-induced oxidation. *Biochemistry* 35: 13112–13117, 1996.
28. Nagababu E and Rifkind JM. Formation of fluorescent heme degradation products during the oxidation of hemoglobin by hydrogen peroxide. *Biochem Biophys Res Commun* 247: 592–596, 1998.
29. Nagababu E and Rifkind JM. Heme degradation during autoxidation of oxyhemoglobin. *Biochem Biophys Res Commun* 273: 839–845, 2000.
30. Nagababu E and Rifkind JM. Reaction of hydrogen peroxide with ferrylhemoglobin: superoxide production and heme degradation. *Biochemistry* 39: 12503–12511, 2000.
31. Nielsen MJ, Moller HJ, and Moestrup SK. Hemoglobin and heme scavenger receptors. *Antioxid Redox Signal*. 2009.
32. Reeder BJ, Sharpe MA, Kay AD, Kerr M, Moore K, and Wilson MT. Toxicity of myoglobin and haemoglobin: oxidative stress in patients with rhabdomyolysis and subarachnoid haemorrhage. *Biochem Soc Trans* 30: 745–748, 2002.
33. Reeder BJ, Svistunenko DA, Cooper CE, and Wilson MT. The radical and redox chemistry of myoglobin and hemoglobin:

from in vitro studies to human pathology. *Antioxid Redox Signal* 6: 954–66, 2004.
34. Reiter CD, Wang X, Tanus-Santos JE, Hogg N, Cannon RO 3rd, Schechter AN, and Gladwin MT. Cell-free hemoglobin limits nitric oxide bioavailability in sickle-cell disease. *Nat Med* 8: 1383–1289, 2002.
35. Rother RP, Bell L, Hillmen P, and Gladwin MT. The clinical sequelae of intravascular hemolysis and extracellular plasma hemoglobin: a novel mechanism of human disease. *JAMA* 293: 1653–1662, 2005.
36. Sadrzadeh SM, Graf E, Panter SS, Hallaway PE, and Eaton JW. Hemoglobin: a biologic Fenton reagent. *J Biol Chem* 259: 14354–14356, 1984.
37. Schaer CA, Schoedon G, Imhof A, Kurrer MO, and Schaer DJ. Constitutive endocytosis of CD163 mediates hemoglobin-heme uptake and determines the noninflammatory and protective transcriptional response of macrophages to hemoglobin. *Circ Res* 99: 943–950, 2006.
38. Schaer DJ, Alayash AI, and Buehler PW. Gating the radical hemoglobin to macrophages: the anti-inflammatory role of CD163, a scavenger receptor. *Antioxid Redox Signal* 9: 991–999, 2007.
39. Schaer DJ, Schaer CA, Buehler PW, Boykins RA, Schoedon G, Alayash AI, and Schaffner A. CD163 is the macrophage scavenger receptor for native and chemically modified hemoglobins in the absence of haptoglobin. *Blood* 107: 373–380, 2006.
40. Schaffner A, Rhyn P, Schoedon G, and Schaer DJ. Regulated expression of platelet factor 4 in human monocytes: role of PARs as a quantitatively important monocyte activation pathway. *J Leukoc Biol* 78: 202–209, 2005.
41. Tolosano E, Fagoonee S, Morello N, Vinchi F, and Fiorito V. Heme scavenging and the other facets of hemopexin. *Antioxid Redox Signal* 2009.
42. Vallelian F, Pimenova T, Pereira CP, Abraham B, Mikolajczyk MG, Schoedon G, Zenobi R, Alayash AI, Buehler PW, and Schaer DJ. The reaction of hydrogen peroxide with hemoglobin induces extensive alpha-globin crosslinking and impairs the interaction of hemoglobin with endogenous scavenger pathways. *Free Radic Biol Med* 45: 1150–1158, 2008.
43. Wojciechowski G, Huang L, and Ortiz de Montellano PR. Autocatalytic modification of the prosthetic heme of horseradish but not lactoperoxidase by thiocyanate oxidation products: a role for heme-protein covalent cross-linking. *J Am Chem Soc* 127: 15871–15879, 2005.

Address correspondence to:
*Dominik J. Schaer, M.D.*
*Department of Internal Medicine*
*University Hospital*
*CH-8091 Zurich, Switzerland*

*E-mail:* dominik.schaer@usz.ch

Date of first submission to ARS Central; August 19, 2009; date of final revised submission, August 23, 2009; date of acceptance, August 23, 2009.

**This article has been cited by:**


1. Harriet Mörtstedt, Marina C. Jeppsson, Giovanni Ferrari, Bo A.G. Jönsson, Monica H. Kåredal, Christian H. Lindh. 2011. Strategy for identification and detection of multiple oxidative modifications within proteins applied on persulfate-oxidized hemoglobin and human serum albumin. *Rapid Communications in Mass Spectrometry* **25**:2, 327-340. [CrossRef]
2. Brandon J. Reeder . 2010. The Redox Activity of Hemoglobins: From Physiologic Functions to Pathologic MechanismsThe Redox Activity of Hemoglobins: From Physiologic Functions to Pathologic Mechanisms. *Antioxidants & Redox Signaling* **13**:7, 1087-1123. [Abstract] [Full Text] [PDF] [PDF Plus]
3. Weiguang Li, Yonghong Wu, Changhong Ren, Yiming Lu, Yan Gao, Xiaofei Zheng, Chenggang Zhang. 2010. The activity of recombinant human neuroglobin as an antioxidant and free radical scavenger. *Proteins: Structure, Function, and Bioinformatics* n/a-n/a. [CrossRef]